

$QQ\bar{q}\bar{q}$ in a chiral constituent quark model

Yue Tan,^{*} Weichang Lu,[†] and Jialun Ping[‡]

*Department of Physics and Jiangsu Key Laboratory for Numerical Simulation of Large Scale Complex Systems,
Nanjing Normal University, Nanjing 210023, P. R. China*

Inspired by Ξ_{cc} reported by LHCb Collaboration and $X(5568)$ reported by D0 Collaboration, the $QQ\bar{q}\bar{q}$ ($Q = c, b$, $q = u, d$) tetraquark states, are studied in the present work. With the help of gaussian expansion method, two structures, diquark-antiquark and meson-meson, with all possible color configurations are investigated systematically in a chiral quark model to search for the possible stable states. The results show that there is no bound state in the isovector $QQ\bar{q}\bar{q}$ system, while there are rather deep bound states in the isoscalar $bb\bar{q}\bar{q}$, $cc\bar{q}\bar{q}$ and $bc\bar{q}\bar{q}$ systems. Mixing two structures of diquark-antidiquark and meson-meson can introduce more attractions and convert some unbound isoscalar states into shallow bound states. The large mass of the heavy quark is beneficial to the formation of the bound state. The separations between quarks are calculated to unravel the spacial structure of the system.

PACS numbers:

I. INTRODUCTION

Since the exotic state $X(3872)$ first observed by Belle collaboration [1], Belle and other collaborations have reported a lot of “ XYZ ” particles [2–4], which stimulated many researches on hadron spectrum. It’s well known that quantum chromodynamics (QCD) is the underlying approach of strong interaction, and in principle QCD allows the existence of exotic states: multiquark states, hybrid states and glueball. However, due to the nonperturbative properties of QCD in the low energy region, it is unavailable for us to use it to study the hadron structures and the hadron-hadron interactions directly. The study of exotic states can provide much essential information, which is absent in the ordinary qqq baryons and $q\bar{q}$ mesons, on low energy QCD.

In 2016, D0 collaboration observed a narrow structure in the $B_s^0\pi^\pm$ invariant mass spectrum with 5.1σ significance. Its mass and width are $M = 5567.8 \pm 2.9^{+0.9}_{-1.9}$ MeV and $\Gamma = 21.9 \pm 6.4^{+5}_{-2.5}$ MeV [5]. Because of the $B_s^0\pi^\pm$ decay mode, $X(5568)$ was interpreted as $sub\bar{d}$ or $sdb\bar{u}$ tetraquark state. But LHCb collaboration got negative result about $X(5568)$ [6]. Nevertheless, the D0 collaborations new result still insisted on the existence of this tetraquark $X(5568)$ [7]. Inspired by the discussions on $X(5568)$, its partner state with quark content $bs\bar{u}\bar{d}$ is proposed afterwards [8, 9]. One year later, LHCb collaboration reported a double charmed baryon Ξ_{cc}^{++} with mass $M = 3621.4 \pm 0.78$ MeV, which 100 MeV heavier than what SELEX collaboration reported [10]. Which is close to our group’s results [11, 12]. The existence of Ξ_{cc}^{++} may imply the existence of the stable $QQ\bar{q}\bar{q}$ system.

Although lacking experimental information regarding to $QQ\bar{q}\bar{q}$ system, theoretical researches on this topic have

a long history [8, 9, 12–22]. Manohar and Wise obtained a weakly bound two-meson state $bb\bar{q}\bar{q}$ using one-pion exchange [13]. Moinester proposed to search for the doubly charmed tetraquarks experimentally as early as the 1990s [15]. Yang *et al.* systematically studied $QQ\bar{q}\bar{q}$ system by using several versions of quark models, and pointed out that iso-scalar $bb\bar{q}\bar{q}$, $cc\bar{q}\bar{q}$ states are deep bound states, and $ss\bar{q}\bar{q}$ states are scattering states [12]. Karliner *et al.* estimated the energy of QQ , Qq and qq from the experimental data of $Q\bar{Q}$, $Q\bar{q}$ and $q\bar{q}$ mesons according to relation between quark-quark and quark-antiquark. Based on this method, they got Ξ_{cc}^{++} ’s mass which was very close to experimental value and predicted the existence of $QQ\bar{q}\bar{q}$ [21]. Eichten *et al.* likened lowest-lying tetraquark configuration as atom (QQ is the “nucleus” while $\bar{q}\bar{q}$ is electron). By heavy-quark symmetry, they predicted that $bb\bar{q}\bar{q}$ must be stable system [22]. Recently Caramés *et al.* got two bound states in the $bc\bar{q}\bar{q}$ system by two different methods [23]. In addition, after replacing $b\bar{q}q\bar{s}$ by $qq\bar{s}\bar{b}$, Chen *et al.* got a bound state in the chiral quark model [8]. Huang *et al.* used quark delocalization color screening model which intermediate-range attraction is provided by quark delocalization and color screening to study $qq\bar{s}\bar{b}$ and $qs\bar{q}\bar{b}$ system, and they found that the tetraquarks composed of $qq\bar{s}\bar{b}$ is more possible to form bound states than the one composed of $qs\bar{q}\bar{b}$ [9]. Very recently, Yang studied $QQ\bar{q}\bar{q}$ system in a chiral quark model by using complex scaling method, several bound states and resonance states were obtained [24].

The QCD inspired quark models successfully describe hadron spectrum, of which the chiral quark model is most popular. In this paper, we use chiral constituent quark model to systematically calculate $QQ\bar{q}\bar{q}$ with the help of gaussian expansion method. Different from the other’s work [21, 22], we consider two kinds of structures, meson-meson and diquark-antiquark, and their mixing. All the possible color and spin configurations are also taken into account. The necessity for mixing the two different structures is that it is not economic way to use

^{*}Electronic address: 181001003@stu.njnu.edu.cn

[†]Electronic address: 161002001@stu.njnu.edu.cn

[‡]Electronic address: jlping@njnu.edu.cn (Corresponding author)

one structure to form a complete set of states because all the possible excited states have to be included. Coupling the important structures to enlarge the model space is a good choice for few-quark systems in the low-energy region. In addition, the root mean square distance between quarks/antiquarks are calculated to unravel the structure of the states if they are bound ones.

The paper is organized as follows. In section II, the chiral quark model and the wave-function of $QQ\bar{q}\bar{q}$ systems are presented. The numerical results are given in Sec. III. The last section is devoted to the summary of the present work.

II. CHIRAL QUARK MODEL AND WAVE-FUNCTION OF $QQ\bar{q}\bar{q}$ SYSTEM

A. Chiral quark model

The chiral quark model has been successful both in describing the hadron spectra and hadron-hadron interactions. The details of the model can be found in Ref. [8, 25–27]. The Hamiltonian of the chiral quark model consists of quarks mass, kinetic energy, and three kinds of potentials, color confinement, one-gluon-exchange and Goldstone boson exchange. The Hamiltonian for four-quark system is written as,

$$H = \sum_{i=1}^4 m_i + \frac{p_{12}^2}{2\mu_{12}} + \frac{p_{34}^2}{2\mu_{34}} + \frac{p_{1234}^2}{2\mu_{1234}} + \sum_{i<j=1}^4 \left(V_{ij}^G + V_{ij}^C + \sum_{\chi=\pi,K,\eta,\sigma} V_{ij}^\chi \right), \quad (1)$$

Where m is the constituent masse of quark(antiquark), and μ is the reduced masse of two interacting quarks or quark-clusters.

$$\mu_{ij} = \frac{m_i m_j}{m_i + m_j}, \quad \mu_{1234} = \frac{(m_1 + m_2)(m_3 + m_4)}{m_1 + m_2 + m_3 + m_4}, \quad (2)$$

and $p_{ij} = \frac{m_j p_i - m_i p_j}{m_i + m_j}$, $p_{1234} = \frac{(m_3 + m_4)p_{12} - (m_1 + m_2)p_{34}}{m_1 + m_2 + m_3 + m_4}$.

The first potential is the color confinement, the quadratic form is used here,

$$V_{ij}^C = (-a_c r_{ij}^2 - \Delta) \lambda_i^c \cdot \lambda_j^c. \quad (3)$$

The second potential is the effective smeared one-gluon exchange interaction,

$$V_{ij}^G = \frac{\alpha_s}{4} \lambda_i^c \cdot \lambda_j^c \left[\frac{1}{r_{ij}} - \frac{2\pi}{3m_i m_j} \sigma_i \cdot \sigma_j \delta(r_{ij}) \right] \quad (4)$$

$$\delta(r_{ij}) = \frac{e^{-r_{ij}/r_0(\mu_{ij})}}{4\pi r_{ij} r_0^2(\mu_{ij})}, \quad r_0(\mu_{ij}) = \frac{r_0}{\mu_{ij}}.$$

TABLE I: Quark Model Parameters ($m_\pi = 0.7$ fm, $m_\sigma = 3.42$ fm, $m_\eta = 2.77$ fm, $m_K = 2.51$ fm).

Quark masses	$m_u = m_d(\text{MeV})$	313
	$m_s(\text{MeV})$	536
	$m_c(\text{MeV})$	1728
	$m_b(\text{MeV})$	5112
Goldstone bosons	$\Lambda_\pi = \Lambda_\sigma(f m^{-1})$	4.2
	$\Lambda_\eta = \Lambda_K(f m^{-1})$	5.2
	$g_{ch}^2/(4\pi)$	0.54
	$\theta_p(^{\circ})$	-15
Confinement	$a_c(\text{MeV})$	101
	$\Delta(\text{MeV})$	-78.3
	$\mu_c(\text{MeV})$	0.7
OGE	α_0	3.67
	$\Lambda_0(f m^{-1})$	0.033
	$\mu_0(\text{MeV})$	36.976
	$\hat{r}_0(\text{MeV})$	28.17

The third potential is the Goldstone boson exchange, coming from the effects of the chiral symmetry spontaneous breaking of QCD in low-energy region.

$$V_{ij}^\pi = \frac{g_{ch}^2}{4\pi} \frac{m_\pi^2}{12m_i m_j} \frac{\Lambda_\pi^2}{\Lambda_\pi^2 - m_\pi^2} m_\pi v_{ij}^\pi \sum_{a=1}^3 \lambda_i^a \lambda_j^a,$$

$$V_{ij}^K = \frac{g_{ch}^2}{4\pi} \frac{m_K^2}{12m_i m_j} \frac{\Lambda_K^2}{\Lambda_K^2 - m_K^2} m_K v_{ij}^K \sum_{a=4}^7 \lambda_i^a \lambda_j^a,$$

$$V_{ij}^\eta = \frac{g_{ch}^2}{4\pi} \frac{m_\eta^2}{12m_i m_j} \frac{\Lambda_\eta^2}{\Lambda_\eta^2 - m_\eta^2} m_\eta v_{ij}^\eta$$

$$[\lambda_i^8 \lambda_j^8 \cos \theta_P - \lambda_i^0 \lambda_j^0 \sin \theta_P],$$

$$V_{ij}^\sigma = -\frac{g_{ch}^2}{4\pi} \frac{\Lambda_\sigma^2}{\Lambda_\sigma^2 - m_\sigma^2} m_\sigma \left[Y(m_\sigma r_{ij}) - \frac{\Lambda_\sigma}{m_\sigma} Y(\Lambda_\sigma r_{ij}) \right]$$

$$v_{ij}^\chi = \left[Y(m_\chi r_{ij}) - \frac{\Lambda_\chi^3}{m_\chi^3} Y(\Lambda_\chi r_{ij}) \right] \sigma_i \cdot \sigma_j,$$

$$Y(x) = e^{-x}/x. \quad (5)$$

In the above formula, σ are the $SU(2)$ Pauli matrices; λ , λ^c are $SU(3)$ flavor, color Gell-Mann matrices, respectively; α_s is an effective scale-dependent running coupling,

$$\alpha_s(\mu_{ij}) = \frac{\alpha_0}{\ln[(\mu_{ij}^2 + \mu_0^2)/\Lambda_0^2]}, \quad (6)$$

All the parameters are determined by fitting the meson spectrum, from light to heavy, taking into account only a quark-antiquark component. They are shown in Table I.

B. The wave-function of $QQ\bar{q}\bar{q}$ system

The $QQ\bar{q}\bar{q}$ system has two structures, meson-meson and diquark-antidiquark, and the wave function of each structure all consists of four parts: orbit, spin, flavor and color wave functions. In addition, the wave function of each part is constructed by coupling two sub-clusters wave functions. Thus, the wave function for each channel will be the tensor product of orbit ($|R_i\rangle$), spin ($|S_j\rangle$), color ($|C_k\rangle$) and flavor ($|F_l\rangle$) components,

$$|ijkl\rangle = \mathcal{A}|R_i\rangle \otimes |S_j\rangle \otimes |C_k\rangle \otimes |F_l\rangle \quad (7)$$

\mathcal{A} is the antisymmetrization operator.

1. orbit wave function

The total wave function consists of two sub-clusters orbit wave functions and the relative motion wave function between two sub-clusters.

$$\begin{aligned} |R_1\rangle &= [[\Psi_{l_1}(\mathbf{r}_{12})\Psi_{l_2}(\mathbf{r}_{34})]_{l_{12}}\Psi_{L_r}(\mathbf{r}_{1234})]_{LM_L} \\ |R_2\rangle &= [[\Psi_{l_1}(\mathbf{r}_{13})\Psi_{l_2}(\mathbf{r}_{24})]_{l_{12}}\Psi_{L_r}(\mathbf{r}_{1324})]_{LM_L} \end{aligned} \quad (8)$$

Where the bracket "[]" indicates angular momentum coupling, and the "L" means total orbit angular momentum coupled by L_r , relative motion angular momentum, and " l_{12} " coupled by " l_1 " and " l_2 ", sub-cluster angular momenta. In addition, we use " $|R_1\rangle$ " denotes meson-meson structure while " $|R_2\rangle$ " denotes diquark-antidiquark structure. In GEM, the radial part of spatial wave function is expanded by Gaussians [28]:

$$R(\mathbf{r}) = \sum_{n=1}^{n_{\max}} c_n \psi_{nlm}^G(\mathbf{r}), \quad (9a)$$

$$\psi_{nlm}^G(\mathbf{r}) = N_{nl} r^l e^{-\nu_n r^2} Y_{lm}(\hat{\mathbf{r}}), \quad (9b)$$

where N_{nl} are normalization constants,

$$N_{nl} = \left[\frac{2^{l+2} (2\nu_n)^{l+\frac{3}{2}}}{\sqrt{\pi} (2l+1)} \right]^{\frac{1}{2}}. \quad (10)$$

c_n are the variational parameters, which are determined dynamically. The Gaussian size parameters are chosen according to the following geometric progression

$$\nu_n = \frac{1}{r_n^2}, \quad r_n = r_1 a^{n-1}, \quad a = \left(\frac{r_{n_{\max}}}{r_1} \right)^{\frac{1}{n_{\max}-1}}. \quad (11)$$

This procedure enables optimization of the ranges using just a small number of Gaussians.

2. spin wave function

Because of no difference between spin of quark and antiquark, the meson-meson structure has the same total

spin as the diquark-antidiquark structure. The spin wave functions of the cluster are shown below.

$$\begin{aligned} \chi_{11}^\sigma &= \alpha\alpha, \quad \chi_{10}^\sigma = \frac{1}{\sqrt{2}}(\alpha\beta + \beta\alpha), \quad \chi_{1-1}^\sigma = \beta\beta, \\ \chi_{00}^\sigma &= \frac{1}{\sqrt{2}}(\alpha\beta - \beta\alpha), \end{aligned} \quad (12)$$

According to Clebsch-Gordan coefficient table, total spin wave function can be written below.

$$\begin{aligned} |S_1\rangle &= \chi_0^{\sigma 1} = \chi_{00}^\sigma \chi_{00}^\sigma, \\ |S_2\rangle &= \chi_0^{\sigma 2} = \sqrt{\frac{1}{3}}(\chi_{11}^\sigma \chi_{1-1}^\sigma - \chi_{10}^\sigma \chi_{10}^\sigma + \chi_{1-1}^\sigma \chi_{11}^\sigma), \\ |S_3\rangle &= \chi_1^{\sigma 1} = \chi_{00}^\sigma \chi_{11}^\sigma, \\ |S_4\rangle &= \chi_1^{\sigma 2} = \chi_{11}^\sigma \chi_{00}^\sigma, \\ |S_5\rangle &= \chi_1^{\sigma 3} = \frac{1}{\sqrt{2}}(\chi_{11}^\sigma \chi_{10}^\sigma - \chi_{10}^\sigma \chi_{11}^\sigma), \\ |S_6\rangle &= \chi_2^{\sigma 1} = \chi_{11}^\sigma \chi_{11}^\sigma. \end{aligned} \quad (13)$$

Where the subscript of " $\chi_S^{\sigma i}$ " denotes total spin of the tetraquark, and the superscript is the index of the spin function with fixed S .

3. flavor wave function

The flavor wave functions of the sub-clusters for two structures are shown below,

$$\chi_{\frac{1}{2}\frac{1}{2}}^{fm} = Q\bar{d}, \quad \chi_{\frac{1}{2}-\frac{1}{2}}^{fm} = -Q\bar{u}, \quad Q = b, c, s \quad (14)$$

$$\chi_{00}^{fd1} = \frac{1}{\sqrt{2}}(\bar{u}\bar{d} - \bar{d}\bar{u}), \quad \chi_{00}^{fd2} = QQ, \quad Q = b, c, s$$

$$\chi_{11}^{fd} = \bar{d}\bar{d}, \quad \chi_{10}^{fd} = -\frac{1}{\sqrt{2}}(\bar{u}\bar{d} + \bar{d}\bar{u}), \quad \chi_{1-1}^{fd} = \bar{u}\bar{u} \quad (15)$$

Where the subscripts of $\chi_{I I_z}^{fm(d)i}$ are the isospin and its third component, and superscripts denote the structure and the index (if needed). The total flavor wave functions can be written as,

$$\begin{aligned} |F_1\rangle &= \chi_0^{fm1} = \frac{1}{\sqrt{2}}(\chi_{\frac{1}{2}\frac{1}{2}}^{fm} \chi_{\frac{1}{2}-\frac{1}{2}}^{fm} - \chi_{\frac{1}{2}-\frac{1}{2}}^{fm} \chi_{\frac{1}{2}\frac{1}{2}}^{fm}), \\ |F_2\rangle &= \chi_1^{fm2} = \chi_{\frac{1}{2}\frac{1}{2}}^{fm} \chi_{\frac{1}{2}\frac{1}{2}}^{fm}, \\ |F_3\rangle &= \chi_0^{fd1} = \chi_{00}^{fd2} \chi_{00}^{fd1}, \\ |F_4\rangle &= \chi_1^{fd2} = \chi_{00}^{fd2} \chi_{11}^{fd}. \end{aligned} \quad (16)$$

Where the subscript of $\chi_I^{fm(d)i}$ is total isospin.

4. color wave function

The colorless tetraquark system has four color structures, including $1 \otimes 1$, $8 \otimes 8$, $3 \otimes \bar{3}$ and $6 \otimes \bar{6}$,

$$\begin{aligned}
|C_1\rangle &= \chi_{1\otimes 1}^{m1} = \frac{1}{\sqrt{9}}(\bar{r}r\bar{r}r + \bar{r}r\bar{g}g + \bar{r}r\bar{b}b + \bar{g}g\bar{r}r + \bar{g}g\bar{g}g \\
&\quad + \bar{g}g\bar{b}b + \bar{b}b\bar{r}r + \bar{b}b\bar{g}g + \bar{b}b\bar{b}b), \\
|C_2\rangle &= \chi_{8\otimes 8}^{m2} = \frac{\sqrt{2}}{12}(3\bar{b}r\bar{r}b + 3\bar{g}r\bar{r}g + 3\bar{b}g\bar{g}b + 3\bar{g}b\bar{b}g \\
&\quad + 3\bar{r}g\bar{g}r + 3\bar{r}b\bar{b}r + 2\bar{r}r\bar{r}r + 2\bar{g}g\bar{g}g + 2\bar{b}b\bar{b}b - \bar{r}r\bar{g}g \\
&\quad - \bar{g}g\bar{r}r - \bar{b}b\bar{g}g - \bar{b}b\bar{r}r - \bar{g}g\bar{b}b - \bar{r}r\bar{b}b), \quad (17) \\
|C_3\rangle &= \chi_{3\otimes \bar{3}}^{d1} = \frac{\sqrt{3}}{6}(rg\bar{r}\bar{g} - rg\bar{g}\bar{r} + gr\bar{g}\bar{r} - gr\bar{r}\bar{g} + rb\bar{r}\bar{b} \\
&\quad - rb\bar{b}\bar{r} + br\bar{b}\bar{r} - br\bar{r}\bar{b} + gb\bar{g}\bar{b} - gb\bar{b}\bar{g} + bg\bar{b}\bar{g} - bg\bar{g}\bar{b}), \\
|C_4\rangle &= \chi_{6\otimes \bar{6}}^{d2} = \frac{\sqrt{6}}{12}(2rr\bar{r}\bar{r} + 2gg\bar{g}\bar{g} + 2bb\bar{b}\bar{b} + rg\bar{r}\bar{g} \\
&\quad + rg\bar{g}\bar{r} + gr\bar{g}\bar{r} + gr\bar{r}\bar{g} + rb\bar{r}\bar{b} + rb\bar{b}\bar{r} + br\bar{b}\bar{r} \\
&\quad + br\bar{r}\bar{b} + gb\bar{g}\bar{b} + gb\bar{b}\bar{g} + bg\bar{b}\bar{g} + bg\bar{g}\bar{b}).
\end{aligned}$$

To write down the wave functions easily for each structure, the different orders of the particles are used. However, when coupling the different structure, the same order of the particles should be used.

5. total wave function

In the present work, $QQ\bar{q}\bar{q}$ and $QQ'\bar{q}\bar{q}$ ($Q' \neq Q$) systems are all investigated. The antisymmetrization operators are different for different systems. For $QQ\bar{q}\bar{q}$ system, we have

$$\mathcal{A} = 1 - (13) - (24) + (13)(24) \quad (18)$$

for meson-meson structure, and

$$\mathcal{A} = 1 - (12) - (34) + (12)(34) \quad (19)$$

for diquark-antidiquark structure. For $QQ'\bar{q}\bar{q}$ system, the antisymmetrization operator becomes

$$\mathcal{A} = 1 - (24) \quad (20)$$

for meson-meson structure, and

$$\mathcal{A} = 1 - (34) \quad (21)$$

for diquark-antidiquark structure. After applying the antisymmetrization operator, some wave function will vanish, which means that the states are forbidden. For example, $IJ^P = 00^+ bb\bar{q}\bar{q}$ state is a forbidden state. All of allowed channels are listed in Table II.

III. RESULTS

In the present calculation, we are interested in the possible bound states. all the angular momenta are set to 0.

TABLE II: All of allowed channels

$QQ\bar{q}\bar{q}$				$QQ'\bar{q}\bar{q}$			
IJ^P	channel	IJ^P	channel	IJ^P	channel	IJ^P	channel
00^+	10^+		1112>	00^+		10^+	1112>
			1122>				1122>
			1212>				1212>
			1222>				1222>
			2144>				2144>
			2234>				2234>
01^+		11^+	1312>	01^+		11^+	1312>
			1322>				1322>
			1411>				1412>
			1421>				1422>
			1511>				1512>
			1521>				1522>
			2343>				2343>
			2433>				2534>
02^+	12^+		1612>	02^+		12^+	1612>
			1622>				1622>
			2634>				2643>
							2634>

The single channel and channel coupling calculations are performed. For the bound state, the root mean square distances between quark-quark/antiquark are also given to unravel the structure of the state.

A. $QQ\bar{q}\bar{q}$ system

In the iso-scalar section, the states with quantum number $IJ^P = 00^+$ and 02^+ are forbidden states, only 01^+ states are allowed. The results for iso-scalar $QQ\bar{q}\bar{q}$ states with $IJ^P = 01^+$ are shown in Tables III and IV. In the table III, the second column gives the energies in the single channel calculation. The third column gives the percentages of each channel for the lowest eigen-state which energy is given in the row marked by “c.c.” in the channel coupling calculation. The last row gives the thresholds for $QQ\bar{q}\bar{q}$ ($Q = b, c, s$) systems.

For $bb\bar{q}\bar{q}$ states, there are three channels have energies lower than the threshold in the single-channel calculation, the lowest one appears in the diquark-antidiquark structure with the light antidiquark being “good antidiquark” [29]. The channel-coupling pushes down the lowest energy 20 MeV and pushes other states above the threshold. The binding energy of the bound state is ~ 311 MeV. The percentages of channels in the lowest eigen-state show that the main component is diquark-antidiquark structure with color configuration $\bar{3} \otimes 3$. The distances between quarks (antiquarks) (see Table IV tell us again that the bound state has diquark-antidiquark structure, $r_{QQ} = 0.3$ fm, $r_{\bar{q}\bar{q}} = 0.4$ fm and $r_{Q\bar{q}} = 0.6$ fm. For $cc\bar{q}\bar{q}$ states, there is one channel has energy lower than the threshold in the single-channel calculation, it is the diquark-antidiquark structure with color configuration $\bar{3} \otimes 3$. The channel-coupling shifts the lowest energy 30 MeV downwards. We obtain the binding energy of the

TABLE III: The energies of iso-scalar $QQ\bar{q}\bar{q}$ ($Q = s, c, b$) system with $IJ^P = 01^+$. “c.c.” stands for channel-coupling.

channel	$b\bar{b}q\bar{q}$		$c\bar{c}q\bar{q}$		$s\bar{s}q\bar{q}$	
1311⟩	10590.2	8.07%	3843.8	9.18%	1410.9	42.92%
1321⟩	10765.6	0.87%	4168.6	0.96%	2060.0	0.08%
1411⟩	10590.2	8.07%	3843.8	9.18%	1410.9	42.92%
1421⟩	10765.6	0.87%	4168.6	0.96%	2060.0	0.08%
1511⟩	10629.6	24.70%	3961.7	9.58%	1830.2	3.94%
1521⟩	10738.3	3.31%	4102.2	3.37%	1903.3	1.03%
2343⟩	10763.2	0.01%	4134.6	0.05%	2048.5	0.57%
2433⟩	10304.6	54.09%	3709.3	66.71%	1636.4	8.46%
c.c.	10282.9		3660.8		1398.6	
Threshold	10600.5		3843.1		1407.7	

bound state ~ 182 MeV. The percentages of channels in the lowest eigen-state and the distances between particles advocate that the dominant structure of the bound state is the diquark-antidiquark structure with color configuration $\bar{3} \otimes 3$. For $s\bar{s}q\bar{q}$ states, all the channels have energies larger than the threshold in the single-channel calculation. However, the channel-coupling plays an important role and it leads to emergence of a bound state, with binding energy ~ 9 MeV. The percentages of channels in the lowest eigen-state and the distances between quarks (antiquarks) claim that the bound state is a molecule, $r_{QQ} = 2.10$ fm, $r_{\bar{q}\bar{q}} = 2.13$ fm and $r_{Q\bar{q}} = 1.58$ fm. One can see that the distance between s and q is larger in four-quark system than that in the meson $Q\bar{q}$. The reason for the large separation is due to the antisymmetrization, If we give up the antisymmetrization, it is reasonable here because the separation between two Q 's (\bar{q} 's) is large, the distance between Q and \bar{q} in one cluster is 0.53 fm. To illustrate the results for $QQ\bar{q}\bar{q}$ ($Q = b, c, s$) systems with $IJ^P = 01^+$, the spacial structures of the systems are shown in Fig. 1. From the figure, we can see that the systems take the 3-dimensional structure, and prefers the diquark-antidiquark structure with $Q = b, c$ (Fig.1(a),1(b)), and the size of the four-quark object increases with the decreasing mass of Q . When the distance between quarks (antiquarks) is larger than the confinement scale (~ 1 fm), the system is transferred to meson-meson structure (Fig. 1(c)). To show what is the critical heavy quark mass for this “phase transition”, the variation of separations between particles with the heavy quark mass m_Q is presented in Fig. 2. The critical heavy quark mass can be read from Fig. 2, $m_Q(\text{critical}) \sim 600$ MeV. It is a second-order phase transition.

To find which interaction leads to the form of bound states, the contribution of each terms in the system hamiltonian to the total energy of the system are tabulated in Table V. The one-gluon-exchange interaction is separated into two terms, color Coulomb (Coul) and

TABLE IV: The distances between particles for the lowest eigen-states of $QQ\bar{q}\bar{q}$ ($Q = s, c, b$) system with $IJ^P = 01^+$ (unit: fm).

	r_{12}	r_{13}	r_{14}	r_{23}	r_{24}	r_{34}
$b\bar{q}b\bar{q}$	0.6	0.3	0.6	0.6	0.4	0.6
$c\bar{q}c\bar{q}$	0.7	0.5	0.7	0.7	0.6	0.7
$s\bar{q}s\bar{q}$	1.58	2.10	1.58	1.58	2.13	1.58

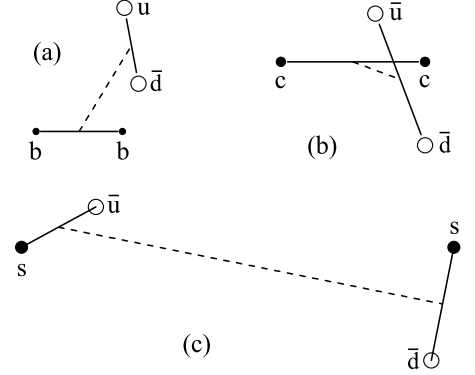


FIG. 1: the spacial structures of $QQ\bar{q}\bar{q}$ system with $IJ^P = 01^+$.

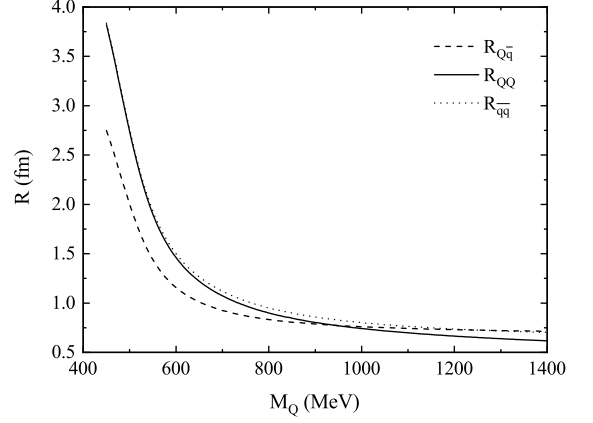


FIG. 2: The variation of the distances between quarks (antiquarks) with the mass of heavy quark.

color magnetic interaction (CMI). V^K makes no contribution to the system which is not listed in the table. From the table, we can see that the major contribution to attraction of the system is from π -meson exchange potential, the major contribution to repulsion is the kinetic energy. Because the compactness increases with

TABLE V: Contributions of each terms in Hamiltonian to the energy of the system. “c.c.” donates the full channel coupling and “t.m.” means the two free mesons. (unit:MeV).

m_Q		T	V^C	V^{Coul}	V^{CMI}	V^π	V^η	V^σ
1400	c.c.	1457.7	-419.6	-648.9	-361.2	-437.1	64.1	-39.0
	t.m.	951.0	-392.1	-631.4	-165.2	0.0	0.0	0.0
	Δ_E	+506.7	-27.5	-17.5	-196.0	-437.1	+64.1	-39.0
800	c.c.	1492.8	-389.3	-675.2	-446.6	-292.1	24.2	-24.1
	t.m.	1203.8	-385.3	-680.6	-375.1	0.0	0.0	0.0
	Δ_E	+289.0	-4.0	+5.4	-71.5	-292.1	+24.2	-24.1
500	c.c.	1583.8	-365.6	-724.5	-654.9	-71.5	-50.8	-6.0
	t.m.	1522.9	-366.3	-728.4	-652.1	0.0	-67.5	0.0
	Δ_E	+50.9	-0.7	+3.9	-2.8	-71.5	-16.7	-6.0

TABLE VI: The energies of iso-vector $QQ\bar{q}\bar{q}$ ($Q = s, c, b$) systems (unit: MeV).

state	IJ^P	c.c.	Threshold	status
$b\bar{b}\bar{q}\bar{q}$	10^+	10561.9	10561.4	ub
	11^+	10600.8	10600.5	ub
	12^+	10639.6	10639.0	ub
$c\bar{c}\bar{q}\bar{q}$	10^+	3725.9	3724.5	ub
	11^+	3844.3	3843.2	ub
	12^+	3962.5	3961.0	ub
$s\bar{s}\bar{q}\bar{q}$	10^+	987.0	983.5	ub
	11^+	1408.9	1407.8	ub
	12^+	1830.5	1827.0	ub

the increase of heavy quark mass, the Goldstone-boson-exchange will become strong when the mass of heavy quark goes high. However, the strong attraction from the Goldstone-boson-exchange will be neutralized by the kinetic energies, which will be more repulsive when the m_Q becomes large. Fortunately the color-magnetic interaction always contributes the sizable attraction for the heavier system, and for the lighter system, other terms, V^η and V^σ supplements the attraction to bind the system.

In the iso-vector section, all the states with quantum number $IJ^P = 00^+, 01^+$ and 02^+ are allowed states. The results of channel coupling calculation are shown in Tables VI. The energies of all the eigen-states are above the thresholds, no bound state is found. Comparing with iso-scalar states, the light antiquark in iso-vector states is “bad antiquark”, the color-magnetic interaction in the one-gluon-exchange is repulsive in this case, which destroy the antiquark structure, so un-binding of states is understandable.

TABLE VII: The energies of iso-scalar $QQ'\bar{q}\bar{q}$ ($Q, Q' = s, c, b$) systems. “c.c.(M-M)”, “c.c.(D-A)” and “c.c.(full)” stand for channel-coupling in meson-meson structure, diquark-antidiquark structure and two structures mixing (unit: MeV).

channel	$bc\bar{q}\bar{q}$		$bs\bar{q}\bar{q}$		$cs\bar{q}\bar{q}$	
$IJ^P = 00^+$						
1111⟩	7139.8	41.02%	5775.5	93.54%	2358.1	95.20%
1121⟩	7518.1	0.10%	6472.6	0.16%	3117.9	0.22%
1211⟩	7295.5	26.92%	6234.6	9.32%	2896.1	0.44%
1221⟩	7346.6	0.16%	6269.4	0.33%	2871.4	0.01%
2133⟩	7011.5	31.64%	6014.6	4.67%	2660.3	3.20%
2243⟩	7426.1	0.16%	6391.2	0.94%	2983.3	0.55%
c.c.(M-M)	7134.1		5774.6		2357.2	
c.c.(D-A)	7005.4		5995.3		2619.1	
c.c.(full)	6965.1		5756.1		2342.1	
Threshold	7143.5		5775.1		2356.8	
$IJ^P = 01^+$						
1311⟩	7259.3	15.26%	6195.6	0.16%	2777.9	0.39%
1321⟩	7517.5	0.01%	6475.8	0.01%	3132.8	0.03%
1411⟩	7179.3	29.95%	5814.4	93.11%	2476.2	94.49%
1421⟩	7521.2	0.01%	6478.0	0.15%	3131.6	0.17%
1511⟩	7298.8	21.11%	6234.7	0.25%	2896.2	0.46%
1521⟩	7431.2	0.01%	6373.3	0.19%	3019.8	0.07%
2343⟩	7479.9	0.00%	6502.7	0.00%	3134.0	0.19%
2433⟩	7022.3	33.22%	6027.9	4.90%	2694.3	3.75%
2543⟩	7453.1	0.01%	6448.2	0.71%	3060.2	0.44%
c.c.(M-M)	7174.5		5813.9		2475.9	
c.c.(D-A)	7020.1		6017.9		2683.5	
c.c.(full)	6983.1		5797.7		2465.3	
Threshold	7182.3		5813.8		2474.7	
$IJ^P = 02^+$						
1611⟩	7297.4	99.67%	6234.0	99.52%	2895.4	99.74%
1621⟩	7625.2	0.06%	6601.7	0.10%	3262.1	0.20%
2643⟩	7502.8	0.28%	6545.5	0.38%	3185.9	0.06%
c.c.(M-M)	7297.4		6233.9		2895.4	
c.c.(D-A)	7502.8		6537.6		3185.9	
c.c.(full)	7296.2		6233.7		2895.2	
Threshold	7300.1		6233.2		2894.1	

B. $QQ'\bar{q}\bar{q}$ system

Because Q and Q' are different quarks and the $QQ'\bar{q}\bar{q}$ system does not have strict symmetry constraint, all the states with possible quantum numbers are all allowed. The results for iso-scalar and iso-vector $QQ'\bar{q}\bar{q}$ states with all possible quantum numbers are given in Tables VII-VIII.

For iso-scalar $bc\bar{q}\bar{q}$ systems, the states with quantum number $IJ^P = 00^+, 01^+$ and 02^+ are all bound states. In the single channel calculation, the meson-meson states

TABLE VIII: The energies of iso-vector $QQ'\bar{q}\bar{q}$ ($Q, Q' = s, c, b$) systems. 'c.c.' stands for full channel coupling (unit: MeV).

state	IJ^P	c.c.	Threshold	status
$bc\bar{q}\bar{q}$	10^+	7144.5	7143.5	ub
	11^+	7183.5	7182.3	ub
	12^+	7301.2	7300.1	ub
$bs\bar{q}\bar{q}$	10^+	5777.1	5775.1	ub
	11^+	5815.9	5813.8	ub
	12^+	6235.3	6233.2	ub
$cs\bar{q}\bar{q}$	10^+	2359.3	2356.8	ub
	11^+	2477.2	2474.7	ub
	12^+	2986.7	2894.1	ub

BD with $J = 0$, B^*D with $J = 1$, B^*D^* with $J = 2$ are bound, and diquark-antidiquark states with “good” antidiquark and $J = 0, 1$ are also bound with even larger binding energies. Other states are all unbound. The channel coupling in one structure lower the energies of the bound states several MeV, generally. For B^*D^* with $J = 2$, the hidden-color channel does not help. The channel coupling with two structures increases the binding energies of the states further. At last the state with $IJ^P = 01^+$ has the largest binding energy, ~ 199 MeV, which is far smaller than that for $bb\bar{q}\bar{q}$ state with $IJ^P = 01^+$, and a little larger than that for $cc\bar{q}\bar{q}$. The phenomenon infers that the attraction, which is provided by the light antiquark, and are almost the same in these systems, the differences come from the kinetic energy terms, where the different masses of heavy quark play a role. The state with $IJ^P = 00^+$ has the second large binding energy, ~ 178 MeV, the states with $IJ^P = 00^+$ and $IJ^P = 01^+$ have the diquark-antidiquark structure, and the state with $IJ^P = 02^+$ is just bound with binding energy ~ 4 MeV, the spacial structure is approaching the molecular one. For iso-scalar $bs\bar{q}\bar{q}$ systems, all the energies of states in single channel calculation are above the corresponding thresholds. For the states with $IJ^P = 00^+$, the channel coupling in meson-meson structure obtains a bound state with binding energy less than 1 MeV, the two structures mixing increase the binding energy to 19 MeV. For the states with $IJ^P = 01^+$, only the channel coupling with two structures obtains a bound state with binding energy 16 MeV. Two states have the molecular structure. For the states with $IJ^P = 02^+$, the

channel coupling is not strong enough to form a bound state. The 00^+ $bs\bar{q}\bar{q}$ state can be a candidate of $X(5568)$ partner, which with four different flavor, but with higher mass, ~ 5775 MeV. For iso-scalar $cs\bar{q}\bar{q}$ systems, we have the similar results with $bs\bar{q}\bar{q}$, only a molecular state with $IJ^P = 00^+$, and a molecular state with $IJ^P = 01^+$, are obtained after all channels in two structures are coupled, the binding energies are ~ 15 MeV and 9 MeV, respectively.

For iso-vector $QQ'\bar{q}\bar{q}$ ($Q, Q' = b, c, s$) systems, all the states are unbound (see Table VIII).

IV. SUMMARY

In the framework of the chiral constituent quark model, the tetra-quark systems with quark contents $QQ(Q')\bar{q}\bar{q}$ are investigated with the help of GEM. All the possible channels and two kinds of structure are coupled to search for bound states. The dynamic calculation show that all the iso-vector $QQ(Q')\bar{q}\bar{q}$ system are scattering states because the isospin vector light antiquark are “bad” ones. In the isospin scalar section, the bound states are abundant. Due to constraint of symmetry, iso-scalar $QQ\bar{q}\bar{q}$ system with $IJ^P = 01^+$ is allowed only. $bb\bar{q}\bar{q}$ and $cc\bar{q}\bar{q}$ are deep bound states with 317.6 MeV and 182.3 MeV binding energy. $ss\bar{q}\bar{q}$ could be a weak bound state with 9 MeV binding energy. On the other hand, for the iso-scalar $QQ'\bar{q}\bar{q}$ system, the constraint of symmetry is released because of the two different heavy quarks, more states are allowed. For the 00^+ states, $QQ'\bar{q}\bar{q}$ states are all bound states, $bc\bar{q}\bar{q}$ is a deep bound state with 178.4 MeV, $bs\bar{q}\bar{q}$ and $cs\bar{q}\bar{q}$ are shallow ones with binding energy 14.7 MeV and 19 MeV, respectively. 01^+ states are similar to 00^+ states, $bc\bar{q}\bar{q}$ is a deep bound state and $bs\bar{q}\bar{q}$ and $cs\bar{q}\bar{q}$ are shallow ones. For 02^+ states, only $bc\bar{q}\bar{q}$ is a weak bound state with 3.9 MeV binding energy, whereas the $bs\bar{q}\bar{q}$ and $cs\bar{q}\bar{q}$ states are all scattering states. Two structures mixing plays an important role in forming the shallow bound states in 00^+ and 01^+ parts.

From our results, we found that the heavy quark mass has great impact on the binding energy in the $QQ(Q')\bar{q}\bar{q}$ system. When the heavy quark mass is more than 1000 MeV, a compact tetraquark can be formed, the π -exchange potential and color magnetic interaction contribute the attraction if the light antidiquark is a “good” antidiquark. While the heavy quark mass is less than 600 MeV, a molecular structure is possible. Is it possible for all light four-quark to form bound states? More calculations are needed.

-
- [1] S. K. Choi *et al.* [Belle Collaboration], Phys. Rev. Lett. **91**, 262001 (2003).
 [2] R. Aaij *et al.* [LHCb Collaboration], JHEP **1907**, 035 (2019).

- [3] M. Ablikim *et al.* [BESIII Collaboration], Phys. Rev. Lett. **110**, 252001 (2013).
 [4] M. Ablikim *et al.* [BESIII Collaboration], Phys. Rev. Lett. **111**, 242001 (2013).

- [5] V. M. Abazov *et al.* [D0 Collaboration], Phys. Rev. Lett. **117**, 022003 (2016).
- [6] The LHCb Collaboration [LHCb Collaboration], LHCb-CONF-2016-004, CERN-LHCb-CONF-2016-004.
- [7] V. M. Abazov *et al.* [D0 Collaboration], Phys. Rev. D **97**, 092004 (2018).
- [8] X. Chen and J. Ping, Phys. Rev. D **98**, 054022 (2018).
- [9] H. Huang and J. Ping, Eur. Phys. J. C **79**, 556 (2019).
- [10] M. Mattson *et al.* [SELEX Collaboration], Phys. Rev. Lett. **89**, 112001 (2002).
- [11] Y. Yang, C. Deng, H. Huang and J. Ping, Mod. Phys. Lett. A **23**, 1819 (2008).
- [12] G. Yang, J. Ping and J. Segovia, Few Body Syst. **59**, 113 (2018).
- [13] A. V. Manohar, M. B. Wise, Nucl. Phys. B **399**, 17 (1993).
- [14] B. Silvestre-Brac and C. Semay, Z. Phys. C **57**, 273 (1993).
- [15] M. A. Moinester, Z. Phys. A **355**, 349 (1996).
- [16] B. A. Gelman, S. Nussinov, Phys. Lett. B **551**, 296 (2003).
- [17] A. Del Fabbro, D. Janc, M. Rosina and D. Treleani, Phys. Rev. D **71**, 014008 (2005).
- [18] Xiao-Hai Liu and Qiang Zhao, J. Phys. G: Nucl. Part. Phys. **36**, 015003 (2009).
- [19] J. Carlson, L. Heller, J. A. Tjon, Phys. Rev. D **37**, 744 (1988).
- [20] J. Vijande, A. Valcarce, K. Tsushima, Phys. Rev. D **74**, 054018 (2006).
- [21] M. Karliner and J. L. Rosner, Phys. Rev. Lett. **119**, 202001 (2017).
- [22] E. J. Eichten and C. Quigg, Phys. Rev. Lett. **119**, 202002 (2017).
- [23] T. F. Caramès, J. Vijande and A. Valcarce, Phys. Rev. D **99**, 014006 (2019).
- [24] G. Yang, J. L. Ping and J. Segovia, Phys. Rev. D **D** 101, 014001 (2020).
- [25] Y. Yang, C. Deng, J. Ping and T. Goldman, Phys. Rev. D **80**, 114023 (2009).
- [26] J. Vijande, F. Fernandez and A. Valcarce, J. Phys. G **31**, 481 (2005).
- [27] X. Chen and J. Ping, Eur. Phys. J. C **76**, 351 (2016).
- [28] E. Hiyama, Y. Kino and M. Kamimura, Prog. Part. Nucl. Phys. **51**, 223 (2003).
- [29] R. Jaffe, Phys. Rep. **409**, 1 (2005).